

Indexed by

Scopus®

## EXPERIMENTAL STUDIES AND MODELLING OF FRACTURE TOUGHNESS OF THE EPOXY SAMPLES WITH ECCENTRIC CRACKS

DOAJ  
DIRECTORY OF  
OPEN ACCESS  
JOURNALS

Crossref

**Vladimir A. Korolenko**  
Moscow Aviation Institute  
(National Research University),  
Institute of General  
Engineering Education,  
Moscow, Russian Federation

**Yulong Li**  
Northwestern Polytechnical  
University (NPU), School of  
Civil Aviation,  
Xi'an Shaanxi, People's  
Republic of China

**Vasiliy N. Dobryanskiy**  
Moscow Aviation Institute  
(National Research University),  
Institute of General  
Engineering Education,  
Moscow, Russian Federation

ROAD  
DIRECTORY OF OPEN ACCESS  
RESEARCH RESOURCES

KoBSON

**Yury O. Solyaev**  
Moscow Aviation Institute  
(National Research University),  
Department of Physical  
Chemistry,  
Moscow, Russian Federation  
Russian Academy of Sciences,  
Institute of Applied Mechanics,  
Moscow, Russian Federation

SCINDEKS  
Srpski citatni indeksGoogle  
Scholar

**Key words:** epoxy resin, stress intensity, fracture criterion, scheme, disruptive load, deformation  
doi:10.5937/jaes0-28162

**Cite article:**

Korolenko, A. V., Li, Y., Dobryanskiy, N. V., & Solyaev, O. Y. [2020]. Experimental studies and modelling of fracture toughness of the epoxy samples with eccentric cracks. *Journal of Applied Engineering Science*, 18(4), 719 - 723.

**Online access** of full paper is available at: [www.engineeringscience.rs/browse-issues](http://www.engineeringscience.rs/browse-issues)

## EXPERIMENTAL STUDIES AND MODELLING OF FRACTURE TOUGHNESS OF THE EPOXY SAMPLES WITH ECCENTRIC CRACKS

Vladimir A. Korolenko<sup>1\*</sup>, Yulong Li<sup>2</sup>, Vasiliy N. Dobryanskiy<sup>1</sup>, Yury O. Solyaev<sup>1,3</sup>

<sup>1</sup>Moscow Aviation Institute (National Research University), Institute of General Engineering Education, Moscow, Russian Federation

<sup>2</sup>Northwestern Polytechnical University (NPU), School of Civil Aviation, Xi'an Shaanxi, People's Republic of China

<sup>3</sup>Institute of Applied Mechanics, Russian Academy of Sciences, Moscow, Russian Federation

The relevance of the work is due to the need for experimental studies to determine the mechanical characteristics of epoxy resin samples, which can be used to check the correctness of the choice of parameters and criteria for the onset of crack growth within the framework of elastic fracture mechanics, cohesive models, models such as virtual crack closure technique, extended finite element method, etc. Thus, the article is aimed at determining the parameters of fracture toughness of samples of brittle epoxy resin with applied eccentric cracks. The leading method for the study of this problem is the experimental method, which makes it possible to determine the critical stress intensity factor for three-point bending of samples with an edge crack, as well as to study samples with an eccentric (relative to the center of the sample) location of cracks. The paper presents the results of experimental studies to determine the critical stress intensity factors for samples of brittle epoxy resin L285 with hardener H 285 (Hexion), obtained without the addition of a plasticizer. The results of testing samples with asymmetric cracks are compared with the results of numerical modeling within the framework of elastic fracture mechanics with the energy fracture criterion. The materials of the article are of practical value, first of all, for the calibration of fracture mechanics models.

*Key words:* epoxy resin, stress intensity, fracture criterion, scheme, disruptive load, deformation

### INTRODUCTION

This paper presents the results of experimental studies to determine the mechanical characteristics of epoxy resin samples, which can be used, first of all, to calibrate fracture mechanics models. Such data are necessary, in particular, to check the correctness of the choice of parameters and criteria for the start of crack growth within the framework of elastic fracture mechanics, cohesive models, models of the VCCT (virtual crack closure technique), XFEM (extended finite element method) type, etc. [1-3].

This work presents detailed data on the geometric parameters of the manufactured samples and the mechanical characteristics of the epoxy resin used. Samples of the material are purposefully obtained without adding any plasticizers to ensure elastic deformation of the samples, in practice, to destruction [4, 5]. Both standard tests to determine the critical stress intensity factor in three-point bending of specimens with an edge crack and tests of samples with an eccentric (relative to the center of the sample) location of cracks were carried out [6]. For such samples, numerical verification calculations were performed using the identified material characteristics and an elastic fracture mechanics model with an energy fracture criterion. Mathematical models for similar problems and experimental studies were investigated in works [7-9].

Calibration of models that allow describing the beginning

of the onset and propagation of damage such as cracks and delamination is important, which is necessary both for characterizing the material under study and for describing the mechanical behavior of structural elements, the loading conditions of which determine the choice of a particular calculation method [10, 11]. From the point of view of strength calculations, the simplest approaches are based on the use of strength criteria. However, these approaches do not give satisfactory results when the model contains stress concentrators in the form of sharp singular angles or cracks. In this case, it is necessary to involve more complex fracture mechanics models, which often contain parameters that require calibration [12-14]. This paper presents the necessary experimental data for the implementation of such works and for further calculations, in particular, those related to the micromechanical modeling of composite materials.

### MATERIALS AND METHODS

For the manufacture of samples, we used L 285 epoxy resin with H 285 hardener (Hexion). The resin components were mixed in proportions of 100: 40, thoroughly mixed, and placed in a vacuum chamber for degassing for 15 minutes at room temperature. After degassing, the mixture was poured into a mold, in which it was cured for 24 hours at a temperature of 50°C. In this way, blanks in the form of plates were made, which were further machined on an axis-controlled mill to obtain a uniform

\*v.korolenko5722-7@national-university.info

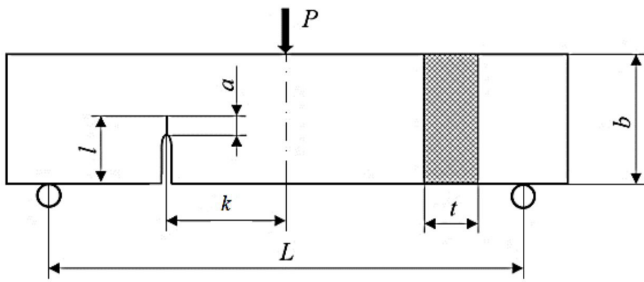


Figure 1: Sample geometry and test pattern

thickness. Experimental flat rectangular samples were cut from the resulting blanks using a cutting machine. The samples were 42 mm long, 4.5 mm thick, and 9.05 (± 0.05) mm high.

Notches were made on the samples on an axis-controlled using a diamond disc. The thickness of the notches was 0.2 (± 0.05) mm. In the top of the notches, natural cracks were created by the impact of the blade with a thickness in the grinding zone <0.1 mm. The geometry and length of the resulting cracks were measured using an Altami Met 5 optical microscope. Five samples with a central location of notches and cracks and 9 specimens with an eccentric location of cracks were made. Eccentric notches and cracks were made with an offset from the center of the sample  $k/L = 0.1; 0.2; 0.3$ . The geometry of the manufactured samples is shown in Figure 1.

The tests were carried out according to the three-point bending scheme using an Instron 5969 universal testing machine. Instron 5969 testing machine designed for static tests and determination of the physical properties of materials for axial tension, compression, bending within the technical capabilities of the machine [15, 16]. The main parts of the machine are the loading device (hydraulic, mechanical) and measuring instruments. The latter register changes in force and deformation. Ovens and cryochambers are used to test materials at temperatures other than normal [17-19]. In the tests, the samples were placed symmetrically on the supports and loaded vertically by loading nose at the central point (Fig. 1) at a speed of 1 mm/s. The distance between the supports was 37 mm. Because of the tests, a load-displacement diagram was constructed. Based on the test results of samples with eccentric cracks, the critical stress intensity factor was determined according to (Eqs. 1-2) (ASTM D5045-14):

$$K_{Ic} = \frac{6P\sqrt{l}}{tb} Y(\lambda) \quad (1)$$

$$Y(\lambda) = 1.93 - 3.07\lambda + 14.53\lambda^2 - 25.1\lambda^3 + 25.8\lambda^4 \quad (2)$$

where  $P$  is the disruptive load,  $l$  is the crack length taking into account the notch,  $b$  is the sample height,  $t$  is the sample thickness,  $\lambda = l/b$  is the ratio of the crack length to the sample height.

In symmetrical samples, notches of various depths were purposefully made to assess the stability of the obtained values of the coefficient  $K_{Ic}$ . Samples with offset cracks were tested in the same way as standard samples.

## RESULTS AND DISCUSSION

Micrographs of cracks created at the top of the notches in the experimental samples are shown in Fig. 2. Diagrams of sample loading obtained as a result of three-point bending tests are shown in Fig. 3. Samples were fractured brittle, into two parts along the direction of crack growth. The diagrams have a linear form, practically, until destruction, which occurred with a complete loss of the bearing capacity of the samples.

The values of the disruptive load for all samples and the values of the critical stress intensity factors calculated by formula (1) for samples with eccentric cracks are presented in Table 1. The values of the notch depth

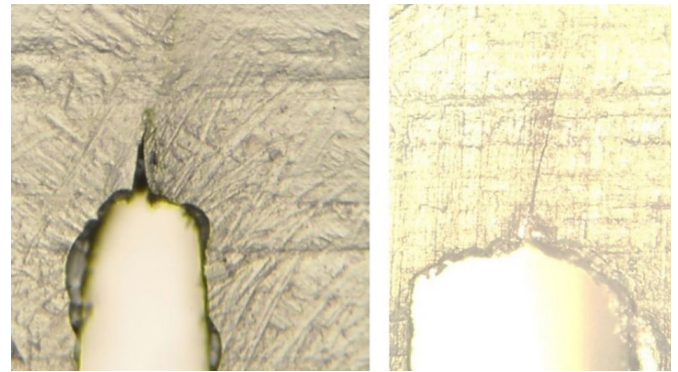


Figure 2: Examples of micrographs of cracks in the top of the notches of the samples

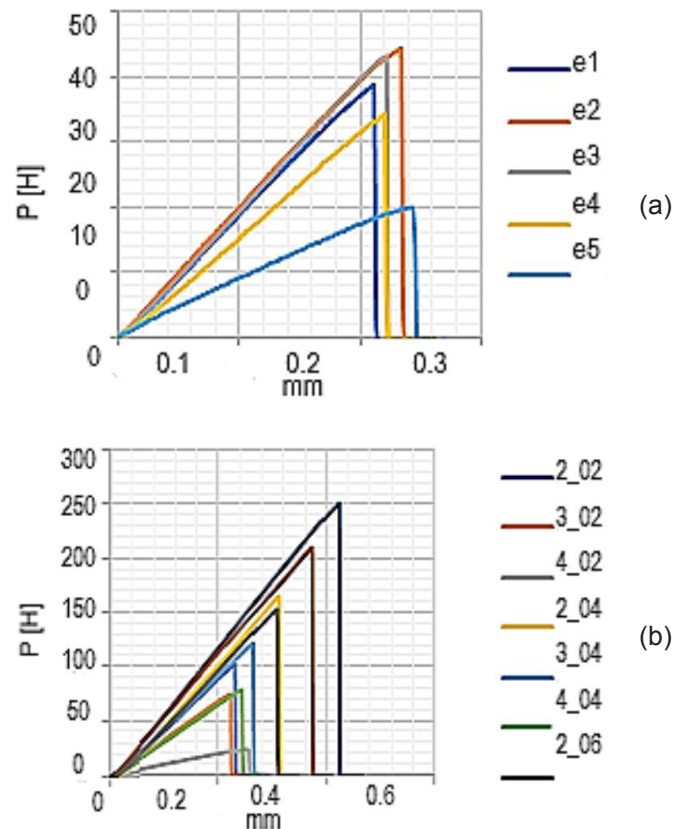


Figure 3: Load-displacement diagrams obtained in tests of samples with central (a) and offset (b) cracks of various lengths

and length of cracks made in experimental samples are also indicated here. The average value of the coefficient  $K_{1c}$  was  $1.2 \text{ MPa m}^{0.5}$ , which is slightly higher than the standard values [20-22], due to the type of epoxy used. Young's modulus of this resin is  $3 \text{ GPa}$ . Poisson's ratio for further calculations is taken equal to  $0.3$ . Tensile/compressive/bending strength:  $75 \text{ MPa}/130 \text{ MPa}/115 \text{ MPa}$ . Strain at break is  $6\%$ .

The test results were compared with numerical finite element modeling. On the basis of calculations for symmetric samples, the critical values of the J-integral ( $J_c$ ) were estimated, from which the values of the critical stress intensity factors were further estimated under the assumption of a plain stressed state  $K_{1c}=(E J_c)^{0.5}$  ( $E$  – Young's modulus) [20, 23]. For asymmetric samples, the critical value of the J-integral was also evaluated based on the

known geometric parameters of the model and the value of the disruptive load established in the experiment.

Numerical calculations were carried out in the Comsol system. An example of a finite element model and a sample loading/fixing scheme are shown in Figure 4. The calculations were carried out in the formulation of a plain stress state under the assumption of small deformations. The J-integral was calculated along a circle enclosing the crack tip with a diameter of no more than  $1/2$  of its length. The notch in the samples was not drawn, since the areas near the crack practically do not participate in the perception of the load, and the presence (or absence) of material in these areas does not significantly affect the calculation results. Thus, in the models, an edge crack with rectilinear edges of the same length as the total length of the notch and crack in the experimental samples was drawn. The initial crack opening in the zone of the lower surface of the sample was set equal to  $10^{-4} \text{ mm}$  (a decrease in this value did not affect the calculation results). The load was set in the center of the upper surface of the model in the form of a uniformly distributed pressure on an area with a length of  $d_0=2 \text{ mm}$ . The supports were modeled by fixing the lower corners of the model according to the hinge-roller scheme.

In numerical calculations, the values of the critical destruction energy were found for all samples (Table 1). The average value for all samples was  $J_c=227 \text{ J/m}^2$  with a standard deviation of  $500 \text{ J/m}^2$ . The average value for samples with symmetrically applied cracks was  $J_c=1053 \text{ J/m}^2$  with a standard deviation of  $437 \text{ J/m}^2$ . It follows from this that, despite a large spread of values, on average, the energy criterion made it possible to accurately assess the bearing capacity of samples with a displaced location of cracks. The values of the stress intensity factor found in the numerical calculation turn out

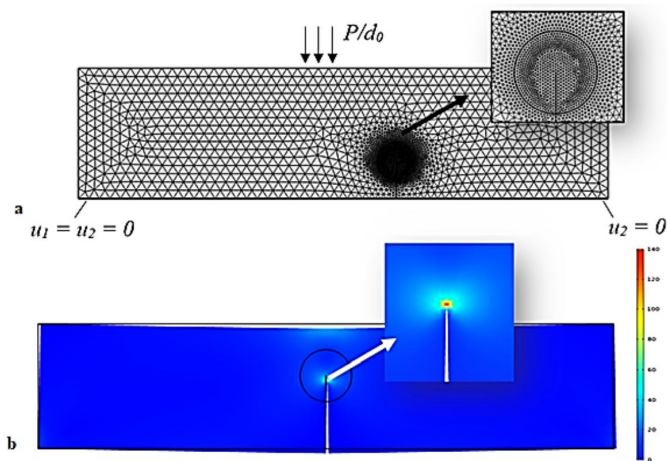


Figure 4: An example of a finite element model used in the calculations (a) and typical calculation results – stress intensity distribution according to von Mises stress in the model (b)

Table 1: Test results for samples made of epoxy resin

No	Crack shift, $k/l$	$l, \text{ mm}$	$a, \text{ mm}$	$P_{max}, \text{ N}$	$K_{1c}, \text{ MPam}^{0.5}$	$K_{1c}, \text{ (FE), MPa m}^{0.5}$	$J_c, \text{ (FE), J/m}^2$
1	0	4.3	0.7	39.0	0.90	1.2	526
2	0	5.0	0.8	44.0	1.25	1.77	1103
3	0	5.3	1.4	43.0	1.37	1.97	1338
4	0	5.1	0.7	34.0	1.06	1.43	712
5	0	6.9	1.2	20.0	1.40	2.17	1590
1_01	0.1	2.6	0.6	104	–	–	793
2_01	0.1	3.7	0.7	75	–	–	938
3_01	0.1	6.9	2.9	22	–	–	1569
1_02	0.2	2.7	0.7	165	–	–	1171
2_02	0.2	3.9	0.9	122	–	–	1772
3_02	0.2	4.5	0.5	79	–	–	1200
1_03	0.3	2.8	0.8	252	–	–	510
2_03	0.3	3.9	0.9	211	–	–	2021
3_03	0.3	4.5	0.5	152	–	–	1937

to be higher than those calculated by the formula (1), which is due, inter alia, to the selected sufficiently wide range of crack lengths that go beyond the limits recommended by the standard.

## CONCLUSIONS

Based on the tests carried out, the parameters of fracture toughness of samples of brittle epoxy resin with applied eccentric cracks were determined. Based on the results of comparing the experiment with numerical calculations, it was found that the average values of the fracture energy in symmetric and asymmetric samples are close and amount to about  $1100 \text{ J/m}^2$ . The scatter of values turns out to be quite large (up to 50%), which is explained by the complex nature of the materials strength and the not quite ideal shape of the applied cracks. Since the material was fragile, the parameters were determined for it, associated only with the onset of the development of defects, which then propagate in a nonequilibrium manner. A small zone of nonlinear deformations can be observed near the maximum load in the presented experimental diagrams; however, from a practical point of view, these small effects can be neglected by applying the corresponding models in an elastic formulation.

The data obtained can be used, for example, for micro-mechanical modeling of composite materials, in which interlaminar cracks are essential from the point of view of the strength and safety of structures. The characteristics of interlaminar strength and fracture toughness are largely determined by the parameters of the composite matrix, which are presented in this work. The coefficient of fracture toughness of inhomogeneous composite materials, generally speaking, can be higher than the coefficient of fracture toughness of the matrix, due to the retardation of crack propagation at the phase interfaces, which can be estimated on the basis of appropriate calculation methods.

## ACKNOWLEDGMENTS

This work was supported by the RFBR grant 18-31-20043.

## REFERENCES

- Allen, R.J., Booth, G.S., Jutla, T. (1988). A review of fatigue crack growth characterisation by linear elastic fracture mechanics (LEFM). Part I – principles and methods of data generation. *Fatigue & Fracture of Engineering Materials & Structures*, vol. 11, no. 1, 45-69.
- Rege, K., Lemu, H.G. (2017). A review of fatigue crack propagation modelling techniques using FEM and XFEM. *Proceedings of the IOP Conference Series: Materials Science and Engineering*, vol. 276, no. 1, 012027.
- Heidari-Rarani, M., Sayedain, M. (2019). Finite element modeling strategies for 2D and 3D delamination propagation in composite DCB specimens using VCCT, CZM and XFEM approaches. *Theoretical and Applied Fracture Mechanics*, vol. 103, no. 102246.
- Godwin, A.D. (2017). *Plasticizers*. William Andrew Publishing, Norwich.
- Nemati Giv, A., Ayatollahi, M.R., Ghaffari, S.H., da Silva, L.F.M. (2018). Effect of reinforcements at different scales on mechanical properties of epoxy adhesives and adhesive joints. *The Journal of Adhesion*, vol. 94, no. 13, 1082-1121.
- Pereira, S.A.G., Tavares, S.M., de Castro, P.M. (2019). Mixed mode fracture: Numerical evaluation and experimental validation using PMMA specimens. *Frattura ed Integrita Strutturale*, vol. 13, no. 49, 412-428.
- Bulychev, N.A., Rabinskiy, L.N. (2019). Surface modification of titanium dioxide nanoparticles with acrylic acid/isobutylene copolymer under ultrasonic treatment. *Periodico Tche Quimica*, vol. 16, no. 32, 338-344.
- Kuznetsova, E.L., Rabinskiy, L.N. (2019). Numerical modeling and software for determining the static and linkage parameters of growing bodies in the process of non-stationary additive heat and mass transfer. *Periodico Tche Quimica*, vol. 16, no. 33, 472-479.
- Skvortsov, A.A., Pshonkin, D.E., Luk'yanov, M.N. (2018). Influence of constant magnetic fields on defect formation under conditions of heat shock in surface layers of silicon. *Key Engineering Materials*, vol. 771, 124-129.
- Skvortsov, A.A., Zuev, S.M., Koryachko, M.V. (2018). Contact melting of aluminum-silicon structures under conditions of thermal shock. *Key Engineering Materials*, vol. 771, 118-123.
- Formalev, V.F., Kolesnik, S.A., Kuznetsova, E.L., Rabinskiy, L.N. (2019). Origination and propagation of temperature solitons with wave heat transfer in the bounded area during additive technological processes. *Periodico Tche Quimica*, vol. 16, no. 33, 505-515.
- Blinov, D.G., Prokopov, V.G., Sherenkovskii, Yu.V., Fialko, N.M., Yurchuk, V.L. (2002). Simulation of natural convection problems based on low-dimensional model. *International Communications in Heat and Mass Transfer*, vol. 29, no. 6, 741-747.
- Talismanov, V.S., Popkov, S.V., Alekseenko, A.L., Zykova, S.S., Karmanova, O.G. (2019). Synthesis of O-[2-(1H-1,2,4-triazol-1-yl)ethyl]phenylthiocarbamate and O-[2-(1Himidazol-1-yl)ethyl]phenylthiocarbamate with fungicidal activity. *International Journal of Pharmaceutical Research*, vol. 11, no. 3, 1237-1240.

14. Babaytsev, A.V., Kuznetsova, E.L., Rabinskiy, L.N., Tushavina, O.V. (2020). Investigation of permanent strains in nanomodified composites after molding at elevated temperatures. *Periodico Tche Quimica*, vol. 17, no. 34, 1055-1067.
15. Kurbatov, A.S., Orekhov, A.A., Rabinskiy, L.N., Tushavina, O.V., Kuznetsova, E.L. (2020). Research of the problem of loss of stability of cylindrical thin-walled structures under intense local temperature exposure. *Periodico Tche Quimica*, vol. 17, no. 34, 884-891.
16. Rabinskiy, L.N., Tushavina, O.V. (2019). Investigation of an elastic curvilinear cylindrical shell in the shape of a parabolic cylinder, taking into account thermal effects during laser sintering. *Asia Life Sciences*, vol. 2, 977-991.
17. Nadirov, R., Syzdykova, L., Zhussupova, A. (2017). Copper smelter slag treatment by ammonia solution: Leaching process optimization. *Journal of Central South University*, vol. 24, no. 12, 2799-2804.
18. Antufev, B.A., Kuznetsova, E.L., Rabinskiy, L.N., Tushavina, O.V. (2019). Investigation of a complex stress-strain state of a cylindrical shell with a dynamically collapsing internal elastic base under the influence of temperature fields of various physical nature. *Asia Life Sciences*, vol. 2, 689-696.
19. Rabinskiy, L.N., Tushavina, O.V. (2019). Problems of land reclamation and heat protection of biological objects against contamination by the aviation and rocket launch site. *Journal of Environmental Management and Tourism*, vol. 10, no. 5, 967-973.
20. Zhu, C.L., Li, J.B., Lin, G., Zhong, H. (2010). Study on the relationship between stress intensity factor and J integral for mixed mode crack with arbitrary inclination based on SBFEM. *Proceedings of the IOP Conference Series: Materials Science and Engineering*, vol. 10, no. 1, 012066.
21. Rodriguez, J., Salazar, A., Gomez, F.J., Patel, Y., Williams, J.G. (2015). Fracture of notched samples in epoxy resin: Experiments and cohesive model. *Engineering Fracture Mechanics*, vol. 149, 402-411.
22. Salazar, A., Patel, Y., Williams, J.G. (2013). Influence of crack sharpness on the fracture toughness of epoxy resins. *Proceedings of the 13th International Conference on Fracture*, vol. 5, 4057-4066.
23. Otarbaev, N.Sh., Kapustin, V.M., Nadirov, K.S., Bimbetova, G.Zh., Zhantasov, M.K., Nadirov, R.K. (2019). New potential demulsifiers obtained by processing gossypol resin. *Indonesian Journal of Chemistry*, vol. 19, no. 4, 959-966.

*Paper submitted: 27.08.2020.*

*Paper accepted: 22.10.2020.*

*This is an open access article distributed under the  
CC BY 4.0 terms and conditions.*